

# Maximal two-layer exchange through a contraction with barotropic net flow

By L. ARMI

Scripps Institution of Oceanography, La Jolla, California 92093

AND D. M. FARMER

Institute of Ocean Sciences, Sidney, BC, Canada, V8L 4B2

(Received 14 January 1985 and in revised form 8 July 1985)

The gravitational exchange of two fluids with different densities between reservoirs connected by a channel of constant depth and slowly varying breadth is analysed as a problem of internal hydraulics. It is shown that maximal two-way exchange with a net barotropic flow requires the presence of two controls, one at the narrowest section and a second or 'virtual' control lying to one side of the narrowest section. The two controls are connected by a subcritical region, but are separated from subcritical conditions in the reservoirs by supercritical flow and stationary internal bores. Solutions are found for maximal exchange without a net barotropic component, in which case the problem is similar to that first examined by Stommel & Farmer (1953). The Stommel & Farmer analysis is shown to be a rather special limiting example of submaximal exchange, not generally applicable to natural flows. The addition of a net barotropic flow yields a range of different flow types, including maximal exchange, one-layer baroclinic flow, one-layer barotropic flow, submaximal flow governed by a reservoir condition and two-layer unidirectional flow. The maximal-exchange solution is integrated for periodic barotropic flow.

---

## 1. Introduction

The gravitational flow of two fluids of differing density through a contraction is important in numerous practical and geophysical problems, including the exchange of water between an estuary and the open sea. A special example of such flows, which has stimulated many recent applications, was first noticed by Stommel & Farmer (1953), who investigated the maximal two-way rate of exchange through a narrow channel connecting a semi-enclosed basin and the ocean. They argued that, beyond a certain point, mixing in a localized area within the basin supplying fresh water increased neither the exchange rate nor the density of the surface layer; they called this limiting example, in which two-layer stratification is maintained within the semi-enclosed reservoir or estuary, 'overmixing'. This seminal contribution turns out to be a very special limiting case of submaximal two-way exchange through a contraction, not generally applicable to many naturally occurring flows. We examine two-way exchanges through a contraction using a more general theoretical framework that includes both the lock exchange and the Stommel & Farmer example and extend the analysis to include barotropic flows, such as those induced by tides or meteorological effects.

We are concerned especially with the limiting hydraulic process that governs maximal two-way exchange of the layers through the contraction. This mechanism

is important in many practical and geophysical problems since it imposes constraints on the rate at which fluids in two connected reservoirs may replace each other. The imposed barotropic flow may be 'moderate', in the sense that both layers move in opposite directions, or it may be 'strong', in which only one layer occurs at the narrowest section. An 'intermediate' condition may also occur, in which one of the layers is motionless within the contraction.

Following a discussion of the basic assumptions and flow configuration in §2, we summarize in §3 the representation of steady two-layer solutions in the Froude-number plane introduced by Armi (1986). In §4 we consider the two-way exchange between two infinite reservoirs and the equivalent problem of exchange between two finite reservoirs that are completely mixed; we also analyse the Stommel & Farmer case in which one reservoir is locally well mixed but maintains a two-layer stratification. The comparison of these cases is made conceptually simpler by discussing a progression of two-way exchange problems, beginning with those in which the flow is less than maximal, proceeding through the Stommel & Farmer case and then on to the exchange between two homogeneous reservoirs.

In §5 we treat moderate barotropic flows and determine the location of the second, or 'virtual', control identified by Wood (1970). Our analysis is extended to strong barotropic forcing in §6; in §7 we discuss the integration of transport applicable to tidal fluctuations. The related, but quite different, problem of two-way exchange over a sill is taken up in the companion paper by Farmer & Armi (1986).

## 2. Basic assumptions and flow configuration

We consider the problem sketched in figure 1 (*a*) of two-layer flow through a channel of slowly varying width connecting two reservoirs. These reservoirs may consist of a semi-enclosed basin on one side, with the ocean on the other. The basin may have a source of positive buoyancy, such as fresh-water run-off in an estuary, or of negative buoyancy, such as high-salinity water produced by evaporation. The latter condition is a common feature of semi-enclosed seas in arid regions, including the Mediterranean (see, for example, Bryden & Stommel 1984; Armi & Farmer 1985) for which reason they are sometimes called inverse estuaries. An important simplification in our analysis, which allows us to isolate the essential physics of the maximal two-way exchange problem, is that the walls of the channel are taken to be vertical. For the same reason we limit our discussion to the flow of two homogeneous layers in the absence of friction. (For an analysis of frictional effects in the exchange problem for the special case of a long strait, see Assaf & Hecht 1974.)

The convention adopted throughout this paper is that for exchange flows the dense water moves from right to left and the less dense water moves from left to right (see figure 1 *a*).

The present study is concerned with the fully nonlinear problem described by the one-dimensional shallow-water equations. The flow in each layer is assumed un-sheared, although this restriction, which has little effect on the results, can be easily removed using energy-distribution coefficients (cf. Chow 1959 p. 28). Hydraulic jumps or other adjustments may occur outside of the neighbourhood of the control (see figure 1 *a*). Although mixing between the layers occurs within the basin, and may also be a prominent feature of the flow outside the control region, we neglect mixing in that short portion of the strait which dominates the hydraulic control.

All of the flows discussed here are steady. Thus our analysis of barotropic flow makes use of the quasi-steady approximation, the validity of which for time-varying

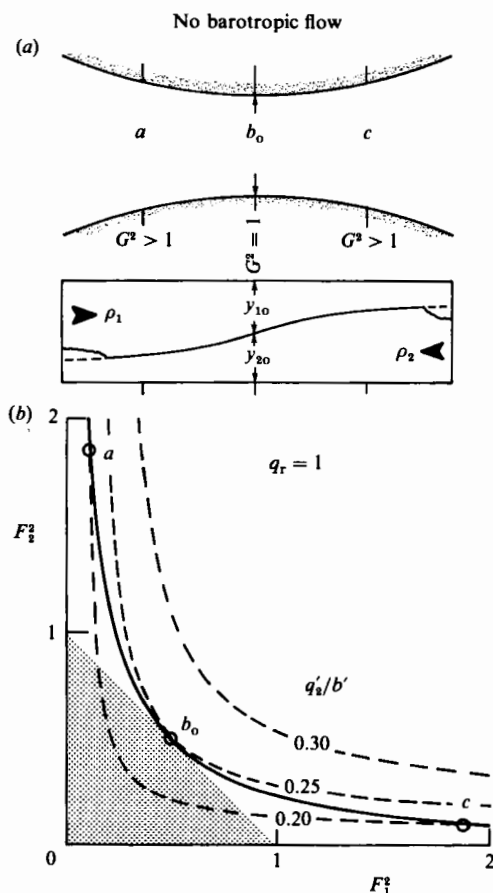


FIGURE 1. (a) Side and plan views for maximal two-layer exchange flow through a contraction with no barotropic flow ( $q_r = 1$ ). (b) Solution curve (solid line) in the Froude-number plane for maximal two-layer exchange flow. Points  $a$ ,  $b_0$ ,  $c$  correspond to locations shown in (a). Dashed curves are contours of normalized flow rate  $q'_2/b'$ . Shaded area represents subcritical flow. Maximal exchange flow in this configuration requires supercritical flow on both sides of  $b_0$ .

flows is commented upon in §7. In the two-layer exchange flows with which we are concerned, the relative density difference between the layers is very much less than that at the free surface. The imposed barotropic flows considered here have external Froude numbers that are very much less than unity so that the free surface may be assumed horizontal. This is often called the rigid-lid approximation and the analysis presented here applies equally to exchange flows beneath rigid lids.

### 3. Two-layer exchange through a contraction and representation in the Froude-number plane

In many straits and channels the shape of the interface along the axis of the flow is asymmetric. Such asymmetry cannot be explained by linear theory for infinitesimal disturbances and we must appeal to the fully nonlinear description provided by the shallow-water equations for which the one-dimensional approximation is applied to each layer. Moreover it can be shown (Armi 1986) that a necessary condition for an asymmetrical interface under steady conditions is that the flow pass through critical

conditions at one or more points in the channel. We use the term ‘critical’ in the hydraulic sense; specifically for two layers, the flow is said to be critical at locations for which

$$G^2 = F_1^2 + F_2^2 = 1 \quad \text{for } g' \ll g, \quad (1)$$

where  $F_i^2 = u_i^2/g'y_i$  is the densimetric Froude number for layer  $i$ ,  $u_i$  is the flow speed,  $y_i$  the layer thickness and  $g' = g\Delta\rho/\rho_2$  is the reduced gravity ( $\Delta\rho = \rho_2 - \rho_1$ ). The upper and lower layers are identified by  $i = 1, i = 2$ , respectively. The composite Froude number  $G^2$  is the parameter which characterizes the essential nonlinearity of the flow.

We therefore choose to express the solutions to the two-layer flow problem in the Froude-number plane ( $F_1^2, F_2^2$ ). In this plane the critical condition represented by (1) collapses to a straight line separating supercritical from subcritical flows. A projection of a solution on to the Froude-number plane is shown in figure 1(b). That portion of the Froude-number plane which is subcritical is shaded.

It is convenient to express the flow rate  $q_i = y_i u_i b$ , where  $b(x)$  is the channel breadth, in non-dimensional form:

$$q'_i = \frac{q_i}{g'^{1/2} b_0 (y_1 + y_2)^{3/2}}. \quad (2)$$

A suitable reference breadth  $b_0$  is the narrowest section of the channel, so that we define the dimensionless breadth  $b'$  as

$$b' = \frac{b}{b_0}. \quad (3)$$

The layer depths  $y_1, y_2$  are non-dimensionalized with respect to the total depth ( $y_1 + y_2$ ) which we take to be constant as discussed above and analysed in detail by Armì (1985 §3):

$$y'_i = \frac{y_i}{y_1 + y_2}, \quad (4)$$

and 
$$y'_1 + y'_2 = 1. \quad (5)$$

From the above definitions of  $q'_i, F_i^2, y'_i, b'$  we express the dimensionless layer depth as

$$y'_i = \left(\frac{q'_i}{b'}\right)^{2/3} F_i^{-2/3}. \quad (6)$$

By convention, flow in the upper layer is taken to be positive and thus, for exchange flows, lower-layer speeds are negative. We define the ratio of flow rates in each layer as  $q_r = q_1 / -q_2$ . In steady flow between two infinite homogeneous reservoirs without a barotropic component,  $q_r = 1$ .

If the flow is steady,  $q_1$  and  $q_2$  do not vary along the channel and (5) and (6) constitute the continuity conditions for each layer. Combining (5) and (6) we can therefore express the continuity equation for each layer in Froude-number space:

$$q_1^{2/3} F_1^{-2/3} + F_2^{-2/3} = \left(\frac{q_2}{b'}\right)^{-2/3}. \quad (7)$$

For a given choice of  $q_r$ , we may solve (7) so as to express the flow rate per unit breadth  $q'_i/b'$  in Froude-number space. Contours of constant  $q'_2/b'$  are plotted as dashed lines in figure 1(b), for  $q_r = 1$ .

The Bernoulli equations for each layer are

$$H_1 = \frac{1}{2}\rho_1 u_1^2 + \rho_2 g(y_1 + y_2) + p, \quad (8)$$

$$H_2 = \frac{1}{2}\rho_2 u_2^2 + \rho_1 g y_1 + \rho_2 g y_2 + p, \quad (9)$$

where  $p$  is the pressure at the surface. Subtracting (8) from (9), dividing through by  $g'\rho_2(y_1 + y_2)$  and making use of the continuity equation, we express the dimensionless Bernoulli equations in Froude-number space:

$$\frac{H_2 - H_1}{g'\rho_2(y_1 + y_2)} = \Delta H' = \frac{F_2^{-2}(1 + \frac{1}{2}F_2^2) - \frac{1}{2}q_1^2 F_1^{-2} F_1^2}{q_1^2 F_1^{-2} + F_2^{-2}}. \quad (10)$$

The term  $\Delta H'$  is the dimensionless energy difference between the two layers. In the absence of internal hydraulic jumps or interfacial or boundary stresses, this quantity is conserved.

If the two-way flow at some point can be specified in terms of  $\Delta H'$ , solutions to (10) of constant  $\Delta H'$  completely define the flow at any point in the absence of a dissipative region such as a hydraulic jump. These solutions have been plotted in detail by Armi (1986).

#### 4. Maximal two-layer exchange flows

We are interested in just one type of solution, corresponding to the maximal two-way exchange. In one example, representing the flow between two infinite reservoirs of uniform but different density, the inflowing layer spreads out in each reservoir so that its thickness becomes negligible. Since the flow rate is finite, the vanishing-layer depth implies a Froude number that is unbounded. Thus the reservoir conditions in this case correspond to  $F_1^2 \rightarrow \infty$  in the reservoir of density  $\rho_2$ , and  $F_2^2 \rightarrow \infty$  in the reservoir of density  $\rho_1$ . There is only one solution to (10) for constant  $\Delta H'$  satisfying these boundary conditions; this is plotted as a solid line in figure 1(b) and it represents the complete solution for the lock-exchange problem ( $\Delta H' = 0.5$ ). The conditions occurring just at the hydraulic control were found by Wood (1970). In figure 1(b), the solid curve connects the boundary conditions specified above. At the narrowest section,

$$F_1^2 = F_2^2 = \frac{1}{2}, \quad (11)$$

$$\frac{q_2'}{b'} = \frac{1}{4}, \quad (12)$$

so that the flow is just critical and the two layers are of equal thickness. If one or both of the reservoirs is not homogeneous, but has two layers ( $\rho_1, \rho_2$ ), the solutions described above may still apply in the neighbourhood of the control. In this situation the subcritical two-layer condition within a reservoir is isolated from conditions in the neighbourhood of the control by an internal hydraulic adjustment or bore (see figure 1a). The necessary conditions for this maximal exchange flow, when one or both of the reservoirs is two-layer, is discussed in §8.

A stable maximal-exchange condition can also be achieved with a reservoir of finite dimensions. This effect can, for example, be achieved by thorough and complete mixing of the inflowing layer within the reservoir away from the control. In this case again, the thickness of the inflowing layer tends to zero. This solution is identical to that for the lock-exchange problem.

The solution shown in figure 1(b) illustrates a fundamental requirement for maximal two-layer exchange that supercritical flow must occur on either side of the control. If supercritical flow occurs on one side of the control only, two-way exchange

will be submaximal. Solutions for maximal and submaximal exchanges are shown in figure 2, together with sketches of the corresponding interface shape.

In the absence of a net barotropic flow the maximal exchange solution ( $\Delta H' = 0.5$ ) is tangent to the control condition,  $G^2 = 1$ , at  $q'_2/b' = 0.25$  (see figure 1*b*). All other solutions that pass through  $G^2 = 1$ , do so at a point for which  $q'_2/b' < 0.25$  and are thus submaximal. Note that the flow-rate curves  $q'_2/b'$  have been omitted from figure 2 for clarity, but are identical to those in figure 1*b*). In figure 2(*a*) the interface shape is sketched for the submaximal exchange corresponding to  $\Delta H' = 0.40$ , with supercritical flow on the left-hand side of the control. In the figure, the supercritical flow is separated from two-layer subcritical flow in the reservoir by a bore. If the reservoir were homogeneous the interface would approach the channel floor. A bore that matches the subcritical conditions in the reservoir to the supercritical flow separating the reservoir from the control will exist provided that the interface height in the reservoir is less than that on the subcritical side. Figure 2(*b*) shows the solution for  $\Delta H' = 0.48$ , which is similar to that in figure 2(*a*) except that the flow rate is greater ( $q'_2/b' = 0.21$ ). When the interface height exceeds 0.5 the reservoir condition which provides the pressure difference to drive the lower layer, changes to the left side. Corresponding submaximal examples are shown in figure 2(*f, g*); the supercritical flow for these examples is on the right-hand side of the control. In figure 2(*a, b*) the lower layer is accelerated to high Froude number on the supercritical side of the control, whereas in figure 2(*f, g*) the upper layer is accelerated to high Froude number.

If the interface height is raised to 0.5 in one reservoir, and dropped to less than 0.5 in the other, two limiting submaximal exchange flows occur. These cases are represented by two segments of the  $\Delta H'$  solutions in figure 2; one segment consists of the straight line intersecting the origin and the other segment consists of one portion of the maximal solution ( $\Delta H' = 0.5$ ). In figure 2(*c*), for which the interface height is  $\Delta H' = 0.5$ , the solution starts with  $F_2^2 \gg 1$  on the left, joins the line through the origin ( $F_1^2 = F_2^2$ ) at the control and proceeds down this line to the origin on the right. To the right of the control the interface must be horizontal. The corresponding example when the interface is 0.5 on the left side is shown in figure 2(*e*).

Finally, in figure 2(*d*), we show the maximal exchange, corresponding to the continuous solution for  $\Delta H' = 0.5$ . In this example, supercritical flow occurs on either side of the control. For the sign convention used in this paper (i.e. the reservoir of dense fluid is on the right), the interface height on the right must be greater than 0.5 and must be less than 0.5 on the left. This is the usual maximal exchange flow, the control condition for which was first identified by Wood (1970). The flow rate for this case,  $q'_2/b' = 0.25$  (cf. equation 12), is identical to that for the limiting submaximal case (figure 2*c, e*). However, it is unlikely that for the limiting submaximal case a flow rate of  $q'_2/b' = 0.25$  could ever be achieved, since this would imply a discontinuous acceleration at the control.

Stommel & Farmer (1953) applied their results to the very peculiar example shown in figure 2(*c*), which they referred to as 'overmixing'. They considered the solution connecting a two-layer finite reservoir to a completely mixed ocean. But they stated that 'the only type of estuary to which the concept of overmixing can be applied is that in which there is vertical stratification' and 'it is important not to attempt to apply this hydraulic condition to vertically mixed estuaries'. Thus they excluded the lock-exchange solution discussed above and shown in figure 2(*d*).

Analysis of the example discussed by Stommel & Farmer (1953) is most easily understood with a progression of solutions as shown above (figure 2*a-d*) corresponding to progressive states of mixing in the finite reservoir or estuary which is connected

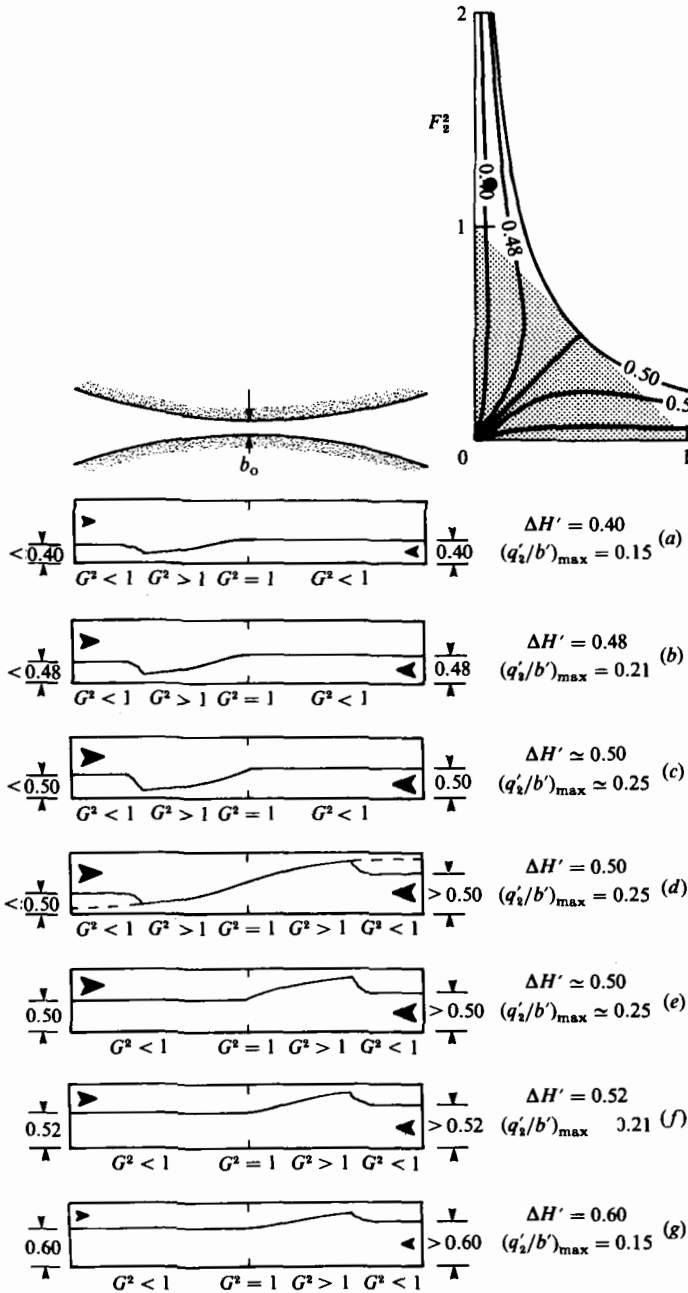


FIGURE 2. (Above) Plan view of contraction and solutions for both maximal and submaximal two-layer flows through a contraction. (Below) Sketches of submaximal (a, b, f, g), limiting submaximal (c, e) and maximal (d) (Wood 1970) two-layer exchange flows. In (a, b) submaximal exchange is controlled by the contraction and the reservoir condition on the right; in (f, g) the contraction and left reservoir condition control the exchange. The interface shape in the limiting examples (c) (Stommel & Farmer 1953) and (e) (Stommel & Farmer 1953, inverted), is controlled by the right- and left-reservoir condition respectively.

to the ocean. Stommel & Farmer describe this progression as follows: 'Suppose that some agency for vertical mixing of the two layers exists in the estuary  $E$  and that the amount of mixing is progressively increased. The upper layer is now somewhat brackish, the discharge of both layers through (the transition)  $T$  is increased, and the interface is nearer to mid-depth. Increased mixing in  $E$  decreases the salinity difference of the two layers at  $T$  and increases the discharge; but there is a point beyond which increased mixing has no further effect on either discharges or the salinities at  $T$ .' Stommel & Farmer described this case, in which mixing proceeded up to the point at which the interface *within the estuary* remained at mid-depth. However, there is no reason why the mixing should not proceed further, to the point where the water within the estuary is thoroughly homogenized. There is no reason why completely mixed estuaries separated from the ocean by a transition should not be entirely analogous to the lock-exchange problem. Thus it seems that the term 'overmixed' has been applied to the special case in which mixing has proceeded just to the point at which the estuary interface is at half depth. Complete mixing is the limiting case applicable to 'well-mixed estuaries' separated from the ocean by a hydraulic transition.

Stommel & Farmer (1953) correctly identified the control condition for maximal exchange and allowed for the possibility of a very weak barotropic component by assuming that the control condition was unaffected. They incorrectly assumed that the interface height must therefore be the same (i.e. 0.5) within the estuary and they therefore limited the application of their result to the very special case shown in figure 2(c). It appears that their laboratory study (Stommel & Farmer 1952) was appropriate only to the study of flow within the transition and not within the estuary. In the more typical lock-exchange problem to which this solution progresses, the interface shape is not restricted in this artificial way, so that the flow converges to the maximal solution sketched in figure 2(d).

## 5. Moderate barotropic flow

In the discussion thus far we have restricted attention to the particular solutions for which the transport in each layer is equal, so that  $q_r = 1$ . If the flow has a net barotropic component, for example due to tides or meteorological effects, or as in Wood's (1970) laboratory experiment, due to differing total-layer depth on each side of the contraction, then  $q_r \neq 1$  and the solutions are skewed in the Froude-number plane. In steady-state solutions with finite reservoirs, buoyancy flux may arise from a local positive or negative mass flux (i.e. river discharge or evaporation), and this mass flux introduces a small barotropic component. This is readily taken into account by choice of the appropriate value of  $U_0$  (see (13*i*) below), but will not normally be a significant factor.

Figure 3 shows the maximal-exchange solution with a barotropic component for the case  $q_r = 0.5$ . As in all examples of moderate barotropic flow the solution connecting the two reservoir conditions intersects the line  $G^2 = F_1^2 + F_2^2 = 1$  twice, once at the narrowest section and a second time at a point lying some distance from the narrowest section in the direction from which the barotropic current is flowing. In particular, the solution ( $\Delta H' = 0.675$ ) which is tangent to the line  $G^2 = 1$  can never connect two reservoirs in the way that it does in the absence of barotropic flow (see figure 4). Thus attempts to determine maximal two-way exchange through the control, by imposing only the constraint that  $G^2 = 1$  (see for example, Murray, Hecht & Babcock 1984) are incorrect. In his analysis of the two-layer lock-exchange



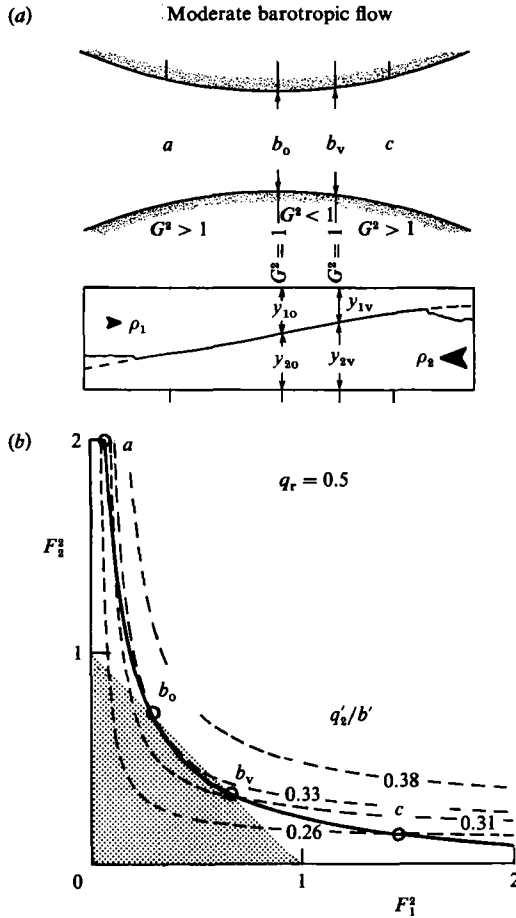


FIGURE 3. (a) Side and plan views for maximal two-layer exchange flow through a contraction with moderate barotropic flow from right to left,  $U_o < 0$ . (b) Solution curve (solid line) in the Froude-number plane for maximal two-layer exchange with  $q_r = 0.5$ . Points  $a, b_o, b_v, c$  correspond to locations shown in figure 3(a). Dashed lines are contours of normalized flow rate  $q'_2/b'$ . Note that the virtual control  $b_v$  is separated from  $b_o$  by subcritical flow.

problem, Wood (1970) recognized that the solution must satisfy  $G^2 = 1$  at two locations in the Froude-number plane; he referred to this 'unknown point' as a virtual control. The virtual control is distinct from the control at the narrowest section and its location is obtained as shown in figure 3.

As the barotropic flow changes, the skew of the solution curves as seen in figure 4 and the relative position of the virtual control changes accordingly so that the latter always lies on the upstream side of the narrowest section, in the sense of the barotropic-flow component. Thus two controls are always required for maximal two-way exchange. Only in the absence of barotropic flow ( $q_r = 1$ ) do these two controls coalesce.

In order to describe all of the flow properties for maximal exchange, both with and without barotropic flow, it is sufficient to solve the equations describing the flow at the two control points. It is convenient to non-dimensionalize all flow speeds in terms of the parameter  $[g'(y_1 + y_2)]^{1/2}$ ; henceforth only non-dimensional equations are used

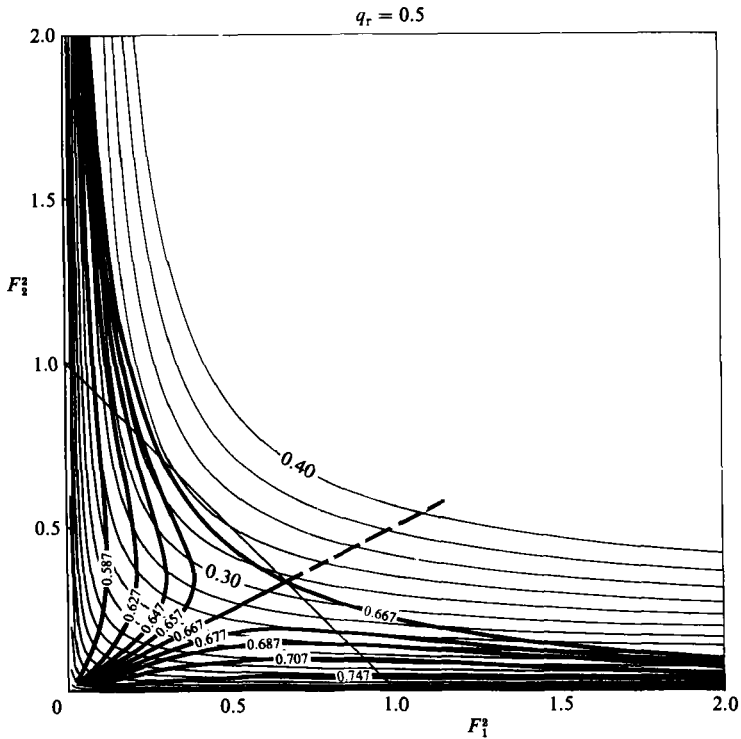


FIGURE 4. Solution curves in the Froude-number plane for  $q_r = 0.5$ , together with normalized flow rates  $q'_2/b'$ .

and we omit the primes. At the narrowest section (subscript  $o$ ), the control condition is

$$\frac{u_{1o}^2}{y_{1o}} + \frac{u_{2o}^2}{y_{2o}} = 1, \quad (13a)$$

and the total depth is

$$y_{1o} + y_{2o} = 1. \quad (13b)$$

At the virtual control (subscript  $v$ ) which has section width  $b_v$  and which is normalized with respect to  $b_o$ , the control conditions are

$$\frac{u_{1v}^2}{y_{1v}} + \frac{u_{2v}^2}{y_{2v}} = 1, \quad u_{1v} + u_{2v} = 0. \quad (13c,d)$$

Equation (13c) corresponds to the intersection of the solutions at  $Q^2 = 1$ . At the virtual control there is an additional constraint: the squares of the flow speeds are equal (Armi 1986 §5 equation 35). For a bi-directional flow this constraint implies that the flow speed in each layer is equal and opposite. Since the total depth at the virtual control is the same as at the narrowest section,

$$y_{1v} + y_{2v} = 1. \quad (13e)$$

We note that (13b) and (13e) imply a level surface, which is justified in our case since the external Froude number is very small. This is quite different to the example studied by Wood (1970) who examined the flow of two moving saline layers beneath a motionless layer of fresh water. In Wood's example the relative density difference

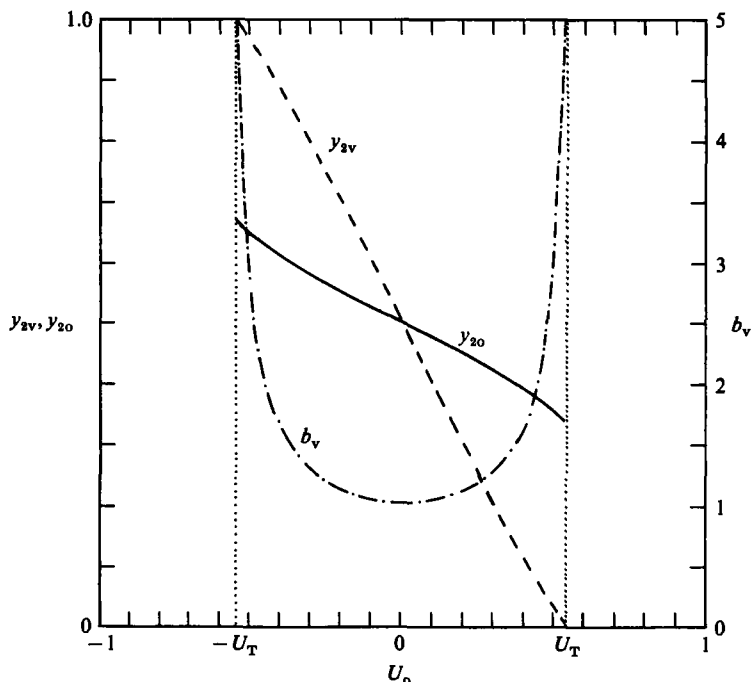


FIGURE 5. Interface height  $y_{20}$  at the narrowest section and at the virtual control  $y_{2v}$ , as functions of  $U_0$  for moderate barotropic flow. The width at the virtual control,  $b_v$ , is also shown.

at the upper interface was not large and the difference in upper interface level between the two reservoirs provided the dynamic head required to drive the flow.

At each of the two controls the relative-energy equation (cf. (10)) is

$$\frac{1}{2}(u_{20}^2 - u_{10}^2) + y_{20} = \frac{1}{2}(u_{2v}^2 - u_{1v}^2) + y_{2v}, \quad (13f')$$

which immediately simplifies, using (13d), to

$$\frac{1}{2}(u_{20}^2 - u_{10}^2) + y_{20} = y_{2v}. \quad (13f'')$$

The continuity equations for each layer are

$$u_{10} y_{10} = u_{1v} y_{1v} b_v, \quad \text{and} \quad u_{20} y_{20} = u_{2v} y_{2v} b_v. \quad (13g, h)$$

The barotropic component is defined by the barotropic flow  $U_0$  at the narrowest section,

$$U_0 \equiv u_{10} y_{10} + u_{20} y_{20}. \quad (13i)$$

The above nine equations (13a-i) are solved for each of the nine unknowns ( $u_{10}$ ,  $u_{20}$ ,  $u_{1v}$ ,  $u_{2v}$ ,  $y_{10}$ ,  $y_{20}$ ,  $y_{1v}$ ,  $y_{2v}$ ,  $b_v$ ) for a given value of  $U_0$ . We now present solutions to these equations for all values of  $U_0$  applicable for moderate barotropic flows.

Figure 5 shows a plot of the interface heights  $y_{20}$ ,  $y_{2v}$  at the narrowest section and at the point of virtual control respectively, together with the width  $b_v$  at the virtual control point. Note that, as  $U_0$  approaches zero, the virtual control coalesces with the control at the narrowest section so that  $y_{20} = y_{2v}$ . As  $U_0$  increases positively, the virtual control occurs at progressively wider points of the contraction on the *upstream* side of  $b_0$ . With increasing  $U_0$  the interface heights at both controls decrease, corresponding to the increased flow rate in the upper layer. These flow rates for each

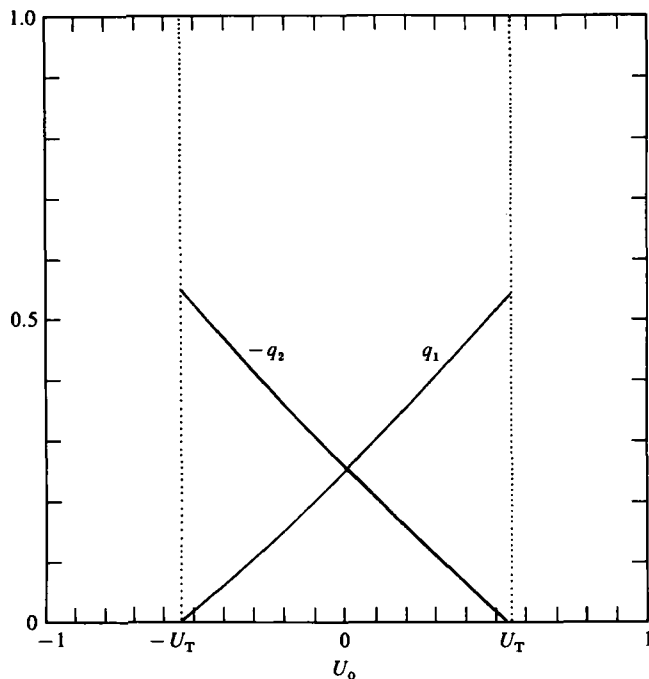


FIGURE 6. Volume flow rates  $q_1$  and  $q_2$  as functions of  $U_o$  for moderate barotropic flows.

layer are plotted in figure 6. The difference in flow rate between layers at any given point in the solution is, of course, just the barotropic component  $U_o$ .

The flow speeds are plotted in figure 7. As anticipated, increasing  $U_o$  results in increasing surface-layer speed and decreasing lower-layer speed at the narrowest section. At the virtual control, which is always on the upstream side, increasing  $U_o$  results in decreasing lower-layer speed, since the virtual control moves to progressively wider points of the channel. In fact the surface-layer speed  $u_1$  and layer depth  $y_1$  at all locations in the control section must increase with increasing barotropic component  $U_o$ . We also plot in this figure the shear  $\Delta u_o$  at the narrowest section. For  $U_o = 0$  this shear is 1 corresponding to marginal stability for long waves (Long 1956). As  $U_o$  increases either positively or negatively, the shear decreases and hence these solutions are all stable.

As mentioned earlier, increasing barotropic flow yields a progressively more skewed set of solutions (see figure 4). This feature is shown quantitatively in figure 8, where we plot the upper-layer Froude numbers  $F_{10}^2$ ,  $F_{1v}^2$  of the two control points as a function of  $U_o$ . The corresponding relative flow rate  $q_r$  is also shown. Figure 8 allows all of the essential features of the maximal two-way solutions such as that shown in figure 4, to be sketched directly for arbitrary barotropic flows.

Maximal exchange with a moderate barotropic flow is sketched in the three central illustrations of figure 9(a). The virtual control is located to the left or right of the narrowest section, depending on the direction of the barotropic component. Similarly, the interface height departs from mid-depth depending on the barotropic flow (see also figure 5).  $G^2 = 1$  at the virtual control and at the narrowest section (figure 9b), which are connected by a subcritical flow. The flow is supercritical on either side of this region. If the barotropic component is great enough ( $U_o = U_T$ ), the upper or lower

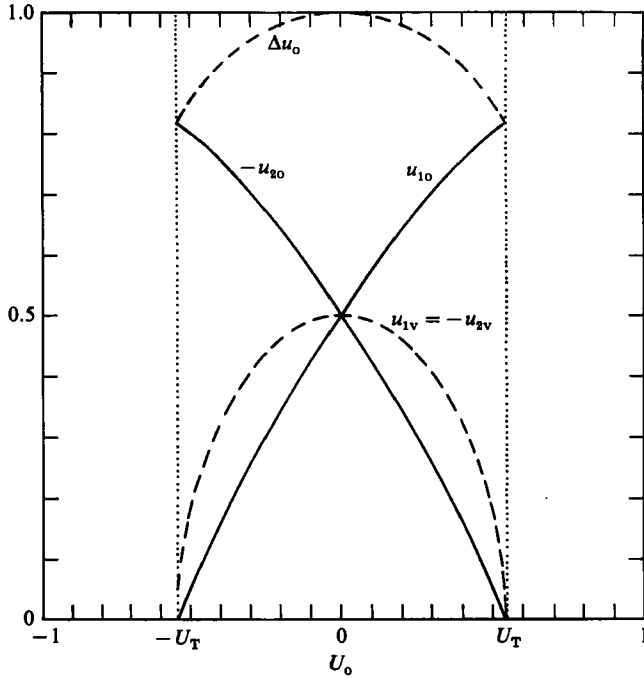


FIGURE 7. Velocities  $u_{10}$ ,  $u_{20}$  at the narrowest section, as well as at the virtual control ( $u_{1v} = -u_{2v}$ ), as functions of  $U_0$  for moderate barotropic flow. Note the velocity difference  $\Delta u_0 = u_{10} - u_{20}$  at the narrowest section is always less than one.

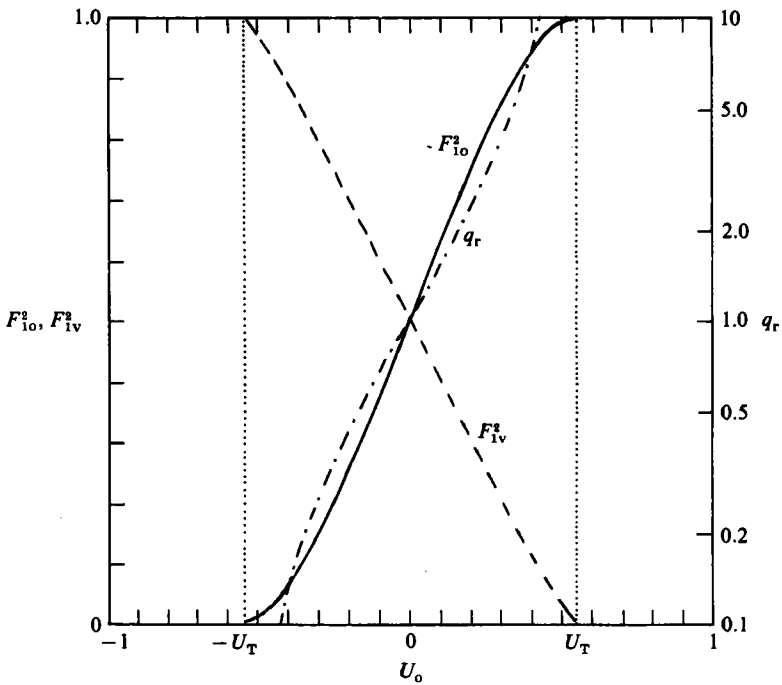


FIGURE 8. Flow-rate ratio  $q_r$  and surface-layer Froude number  $F_{10}^2$  at the narrowest section, and at the virtual control,  $F_{1v}^2$ , as functions of  $U_0$  for moderate barotropic flows.

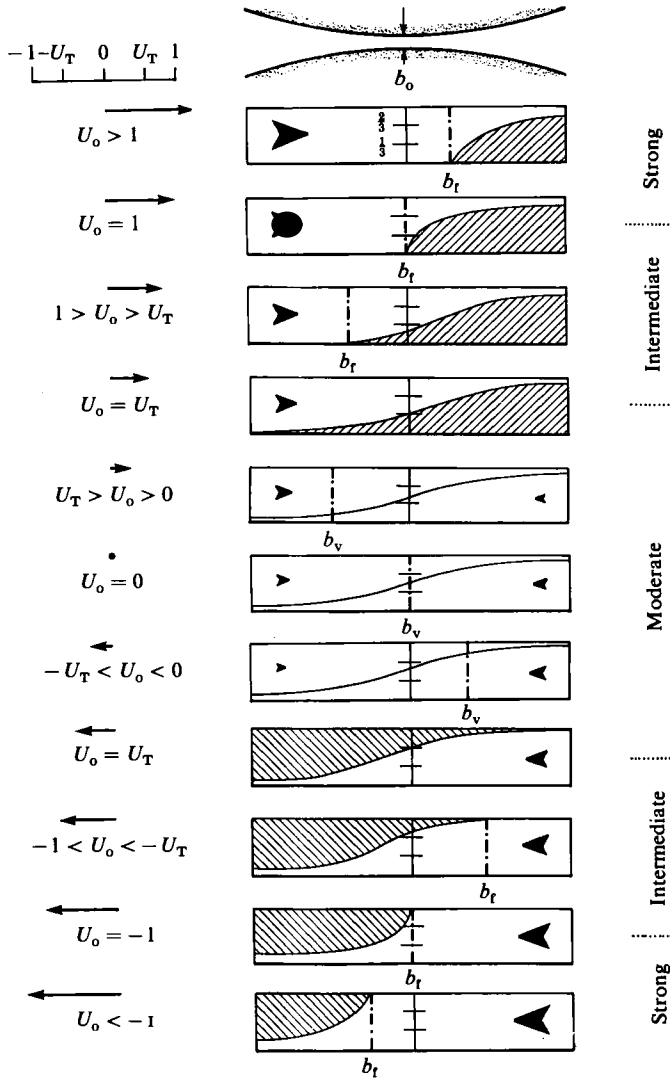


FIGURE 9(a). For caption see facing page.

layer is arrested and the exchange is controlled only at the narrowest section. The virtual control has effectively disappeared into the reservoir on the side from which the barotropic flow emanates. The control in this case separates critical flow in one reservoir from subcritical flow in the other, the direction of the barotropic component determining the orientation of the transition.

### 6. Intermediate and strong regimes: box flows and the frictionless salt wedge

When the barotropic flow reaches the value  $U_o = U_T$  (evaluated below, equation (17)), a transition occurs between two-way exchange and single-layer flow. The motionless layer, which is shaded in figure 9, does not enter the dynamics except insofar as it determines the reduced gravity.

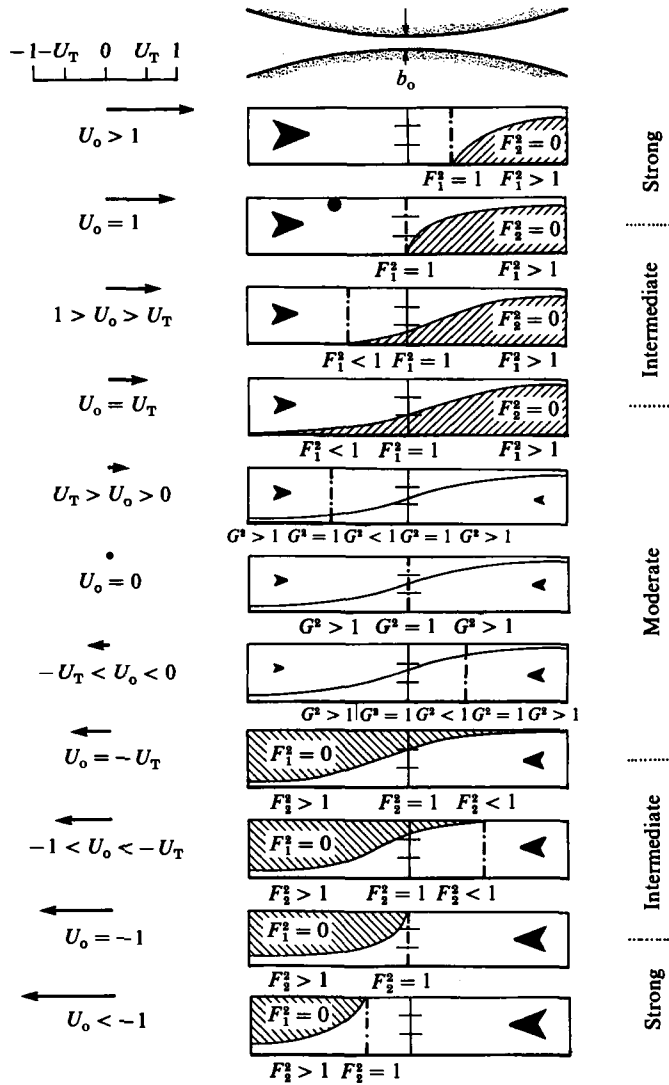


FIGURE 9. (a) Sketches of the interface positions as a function of barotropic flow  $U_0$ . The arrows to the left of the sketches indicate the strength and direction of the barotropic component; the arrowheads within each sketch indicate the strength and direction of flow rate for each layer. Motionless layers are shaded. The positions of the virtual control  $b_v$  and the location of the front  $b_f$  are shown beneath the appropriate sketches. (b) Sketches of interface position as a function of barotropic flow  $U_0$ , identical to (a), showing layer Froude numbers and composite Froude numbers at different positions, beneath the appropriate sketches.

Consider first the example of  $U_0 = -U_T$  shown in figure 9. This single-layer flow is identical to open-channel flow through a contraction starting from the same reservoir depth, except that  $g$  is replaced by the corresponding value of  $g'$ . Note that, as in open-channel flow, the interface height at the narrowest section is  $\frac{2}{3}$  (see also figure 5). The flow is subcritical upstream ( $F_2^2 < 1$ ), critical at the narrowest section ( $F_2^2 = 1$ ) and supercritical downstream ( $F_2^2 > 1$ ). The example of  $U_0 = U_T$  is inverted but otherwise identical to  $U_0 = -U_T$  since in this case it is the upper layer that flows.

For  $U_0$  in the ranges  $-1 < U_0 < -U_T$  and  $1 > U_0 > U_T$ , which we refer to as

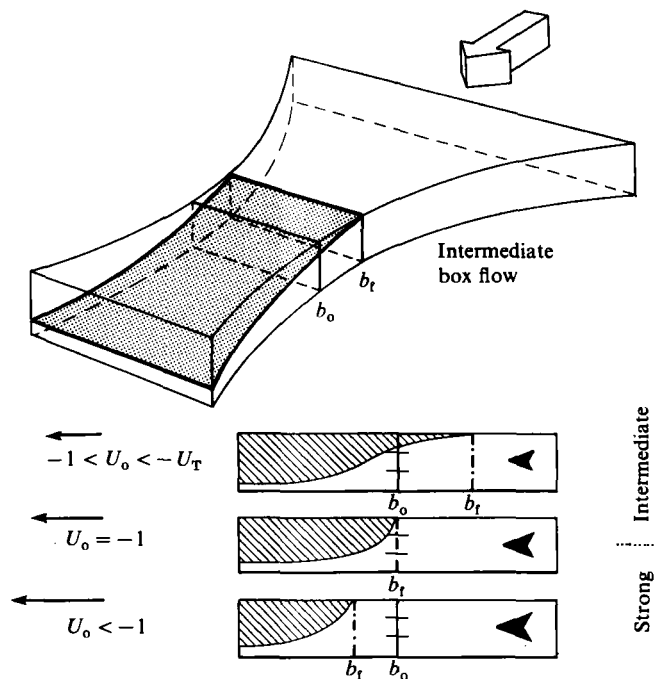


FIGURE 10. Sketches of box flows. *Above*: perspective view of intermediate box flow in which the interface meets the surface upstream of the narrowest section. *Below*: sketches of intermediate, transitional and strong box flows.

intermediate barotropic flow, the interface intersects the surface or bottom respectively, not in the reservoir as in the limiting case  $U_o = -U_T$  or  $U_o = U_T$ , but within the contraction.

Flows in the range  $U_o < -U_T$  are identical to flow of a single layer through a contraction with rigid, flat, upper and lower surfaces. We refer to these as 'box flows', sketches of which are shown in figure 10. For  $-1 < U_o < -U_T$  the interface reaches the upper surface of the box upstream of the narrowest section. The flow rate  $U_o$  determines the interface height at the control point  $b_o$ . For  $U_o < -U_T$  this height exceeds  $\frac{2}{3}$  of the box depth and hence the subcritical region upstream of the control cannot extend into the reservoir and will intersect the surface some short distance upstream of the narrowest section. For progressively greater flow rate  $U_o$ , the intersection lies closer to the narrowest section, which it reaches for  $U_o = -1$ . For this flow rate the critical depth at  $b_o$  is equal to the box depth and there is no longer any upstream influence of the control. Conditions downstream of the narrowest section are determined by control at  $b_o$ . For  $U_o < -1$  the control point, and hence the intersection  $b_t$ , lies downstream of  $b_o$ .

The examples of intermediate and strong barotropic flow ( $U_o \geq U_T$ ) shown in the upper four sketches of figure 9 are inverted but otherwise identical to  $U_o \leq -U_T$ , since in this case it is the upper layer that flows. Inverted box flows of this type have a common geophysical analogy in the frictionless salt wedge at the mouth of an estuary, for which the salt-wedge position is determined by the channel width and the flow rate. The dynamics in this case differ from those normally assumed to hold when the wedge has advanced up a long, uniform channel and the interface shape and position is influenced by friction and entrainment (cf. Dyer 1973).



Box flows are quite different to gravity currents or to the advance of an empty cavity along the upper boundary of a liquid, as discussed by Benjamin (1968). Box flows are steady with respect to the contraction. Gravity currents and cavity flows can only be considered steady in a coordinate frame that moves along with the front. This distinction is important, since, in contrast to gravity currents, the frontal boundary for box flows is stationary and the interface shape behind the front is determined by flow rate and channel width.

Over the range  $|U_T| < |U_0| < 1$  corresponding to intermediate barotropic flow, in which the front lies upstream of  $b_0$ , we determine the solutions as follows. From the control condition (13a) and the definition of  $U_0$  in (13i) we find for a single moving layer

$$u_{i0} = U_0^{\frac{1}{3}}, \quad (14)$$

$$y_{i0} = U_0^{\frac{2}{3}}, \quad (15)$$

where the subscript  $i$  refers to the single moving layer. Eliminating  $u_{i0}$ ,  $y_{i0}$  from the energy equation (13f'), and making use of the identity  $U_0 = b_f u_{if}$ , yields

$$\frac{3}{2}U_0^{\frac{2}{3}} = \frac{1}{2}\frac{U_0^2}{b_f^2} + 1. \quad (16)$$

This result allows us to evaluate  $U_T$ , which is the limiting case for  $b_f \rightarrow \infty$ :

$$U_T = \left(\frac{2}{3}\right)^{\frac{3}{2}} = 0.544. \quad (17)$$

from (16) we also solve for the breadth of the channel at the front,  $b_f$ ,

$$b_f = U_0(3U_0^{\frac{2}{3}} - 2)^{-\frac{1}{2}}. \quad (18)$$

When  $|U_0| = 1$  the front lies at the narrowest section ( $b_f = b_0$ ) where the flow is just critical ( $F_i^2 = 1$ ).

The slope of the front is given by

$$\frac{\partial y_i}{\partial x} = \frac{F_i^2}{1 - F_i^2} \frac{y_i}{b} \frac{db}{dx} \quad (19)$$

(Armi 1985 equation 11c), where  $i$  is the moving layer. The front first appears in the appropriate reservoir (refer to figure 9a, b) when  $|U_0| = U_T$ . Here both  $F_i^2 \ll 1$ , and  $y_i/b \ll 1$ ; hence the slope of the front is very slight,  $\partial y_i/\partial x \ll db/dx$ . The slope remains small for intermediate barotropic flows since  $db/dx \ll 1$  by our assumption of slowly varying flow.

For  $|U_0| > 1$  critical conditions (i.e. (14) and (15)) can no longer be satisfied at the narrowest section, which is then filled with a single moving layer. We refer to this condition as strong barotropic flow. Downstream of the narrowest section the flowing layer decelerates and at some width  $b_f$  reaches critical conditions:

$$F_i^2 = 1. \quad (20)$$

With strong barotropic flow ( $F_i^2 \sim 1$ ), the frontal slope becomes steep and non-hydrostatic effects need to be included to describe details of the frontal shapes which are only shown schematically in figure 9(a, b).

Solutions for the three barotropic regimes, moderate, intermediate and strong, are shown in figures 11–13. In figure 11 we show the interface height  $y_{20}$  at the narrowest section and the breadth of the channel  $b_f$  at the front location. The interface height varies smoothly over the range  $-1 < U_0 < 1$ , but  $b_f$  is a very sensitive function of  $U_0$  for  $U_0$  close to  $U_T$ . We anticipate that, in naturally occurring two-layer flows

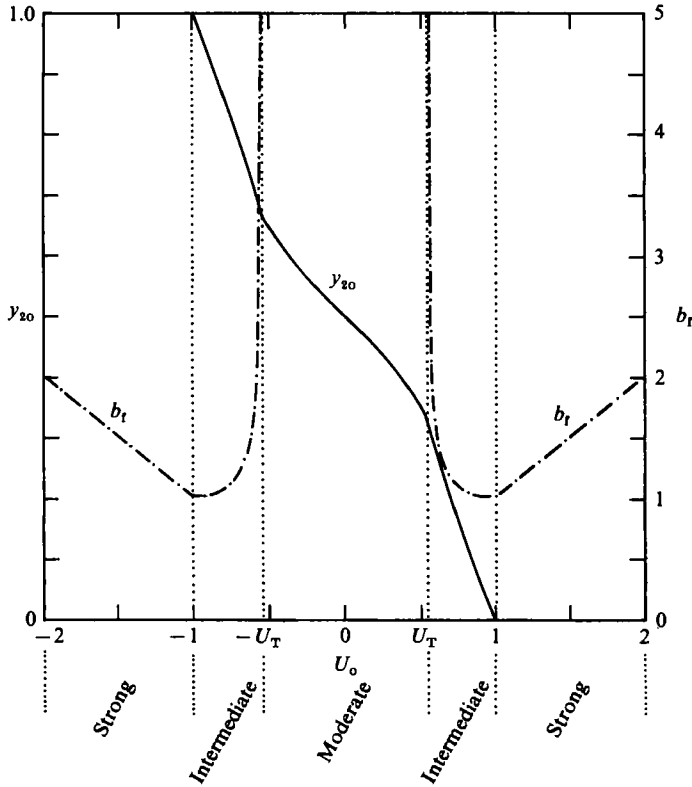


FIGURE 11. Interface height  $y_{20}$  and channel width  $b_f$  at the transition between single and two-layer fluid, for intermediate and strong barotropic flow.

subject to tidal forcing, fronts will appear quite suddenly just upstream of the narrowest section with increasing flow. Once the front has been swept downstream of  $b_o$ , the corresponding channel width  $b_f$  varies linearly with the barotropic flow  $U_o$ , determined by (20) together with the continuity equation

$$b_f = U_o. \tag{21}$$

The same relationship holds for the intersection point  $b_f$  in a box flow.

The flow rates  $q_1, q_2$  for each layer are shown in figure 12. Beyond the transition  $U_T$ , only one layer is moving so that for this layer  $q_i = U_o$ ; two-way exchange is limited to the range of moderate flows ( $|U_o| < |U_T|$ ). Figure 13 shows the flow speeds, both at the narrowest section ( $u_{10}, u_{20}$ ) and also, for the moving layer, at the frontal location  $u_{1f}, u_{2f}$ . If the front has moved past the narrowest section,  $u_{i0} = U_o$ . The flow speed at the front ( $u_f = U_o/b_f$ ), however, is sensitively dependent on  $U_o$  for  $U_o < 1$ . For the intermediate range  $|U_T| < |U_o| < 1$ ,  $F_{i0}^2 = 1$ , since control is maintained with only one moving layer. If  $|U_o| > 1$ , internal hydraulic control is lost at the narrowest section which is then filled with a single flowing layer.

For intermediate flow the stability parameter  $\Delta u$  is equal to  $u_i$  since there is only a single moving layer. These flows are always stable in the neighbourhood of the control. However, outside of the control region there will be a point or points in the supercritical region, for all of the examples shown in figure 9, at which the flow

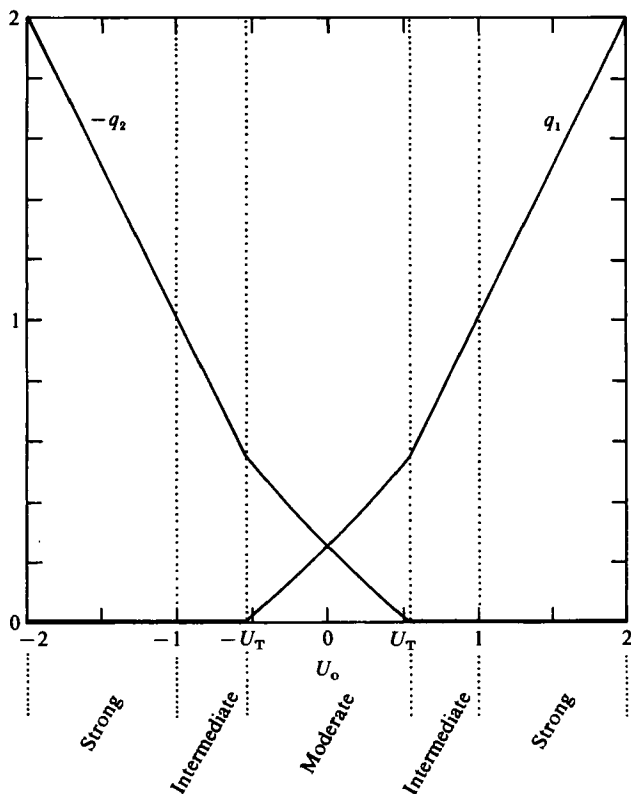


FIGURE 12. Flow rates  $q_1$ ,  $q_2$  for moderate, intermediate and strong barotropic flow.

becomes unstable according to Long's criterion. But this instability does not directly influence the control and is not relevant to the maximal-exchange flows discussed here.

### 7. Influence of periodic flows on maximal two-way exchange

In addition to the baroclinic exchange described earlier, natural flows in channels and straits may also include periodic components associated with tides. Provided that the tidal effect is slow relative to the time taken for interfacial adjustment, we may treat the flow as quasi-steady. More specifically, this restriction implies that for moderate barotropic flow the time for a long wave to propagate through the subcritical section between the two controls ( $b_o$ ,  $b_v$ ) must be short compared with the tidal period.

Tidal flow will always tend to increase the maximal two-way exchange. This is self-evident for the intermediate and strong regimes, in which cases the internal hydraulic control of the exchange is lost so that only a single layer flows (see figure 12). The effect is weaker, though still present, in the moderate regime (figure 6) for which  $q_i(U_o)$  departs only slightly from straight lines.

The integrated influence of flow over a tidal period is illustrated in figure 14. For  $U_{\max}$  greater than  $U_T$ , the mean transport  $\langle \bar{q} \rangle$  approaches a line of slope  $\pi^{-1}$ .

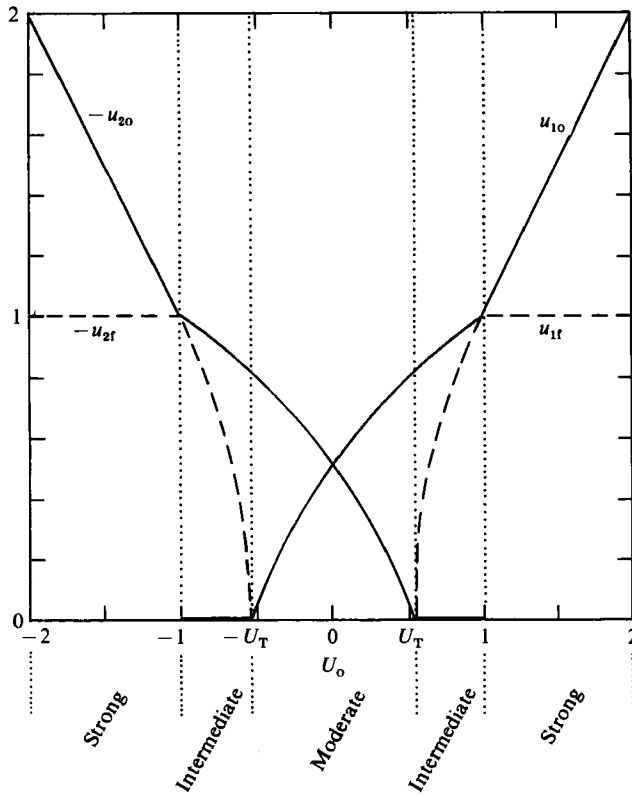


FIGURE 13. Layer speeds  $u_{10}$ ,  $u_{20}$  at the narrowest section  $b_0$ , and layer speeds  $u_{1f}$ ,  $u_{2f}$  at the transition between single and two-layer conditions.

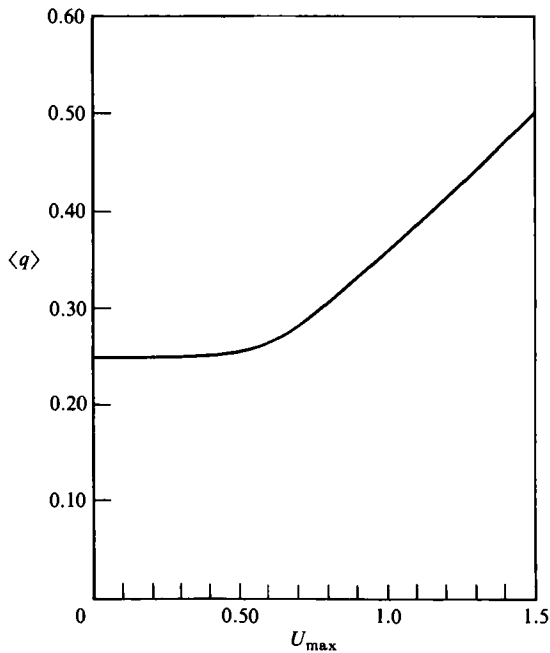


FIGURE 14. Exchange rate  $\langle q \rangle$  averaged over a tidal cycle of amplitude  $U_{\max}$ .

## 8. Conclusion

Two-way exchange through a horizontal contraction is a common natural phenomenon wherever the water on each side is of different density. We have discussed the behaviour of this exchange in the limit when the internal hydraulic conditions fully determine the two-way exchange and have shown how these are modified by barotropic flow. However, it may happen that with barotropic forcing, for example during some portion of a tidal period, submaximal exchange occurs. Submaximal exchange will always be influenced by one of the reservoir conditions; this possibility is discussed in the Appendix.

Although this problem was introduced over thirty years ago by Stommel & Farmer (1953), it appears that the original analysis applies only to a very special example, which will not normally occur in nature. Moreover this important contribution, though widely quoted in the literature, has generally been misunderstood and incorrectly applied; it represents an interpretation of conditions only at the control and fails to distinguish between the limiting submaximal- and the usual maximal-exchange flows. The Stommel & Farmer example has also been incorrectly applied to two-way exchange over a sill. As discussed by Farmer & Armi (1986), hydraulic control of two-way exchange over a sill is fundamentally different to flow through a horizontal contraction; in particular the steady solution between two mixed reservoirs does not satisfy the relationship  $y_{10} = y_{20} = \frac{1}{2}$ .

It is appropriate to consider also the problem of control in the case of more than one channel connecting the two reservoirs. The two-way exchange in this situation is readily found by summing the exchange for each individual channel, since the behaviour at each control is determined solely by the local channel width and by the density difference between reservoirs.

The analysis has identified the essential features governing two-way exchange through a horizontal contraction. It has been shown that, in the general case of barotropically forced steady two-way exchange, maximal flow requires the existence of two controls, one at the narrowest section ( $b_0$ ) and a second 'virtual' control ( $b_v$ ) lying upstream of  $b_0$ . Between these locations subcritical flow connects the two controls. Outside of the control region the flow is supercritical, thus isolating the two-way exchange in the control region from the influence of the reservoirs. Thus maximal two-way exchange is governed solely by the geometry of the channel and the densities of the two fluids. In the absence of barotropic flow the two controls coalesce at the narrowest section ( $b_0$ ).

If a reservoir is not homogeneous, a stationary bore matches the supercritical conditions near the control to the subcritical conditions in the reservoir. Maximal two-way exchange with a two-layer reservoir is only possible if the interface height in the reservoir lies within a range that permits the existence of this bore, cf. Appendix, equation (A 1). For reservoir heights outside this range the exchange is submaximal and is determined both by the single control ( $b_0$ ) and by the reservoir condition.

If the barotropic forcing is sufficiently strong, two-way exchange can be arrested: only a single layer then flows through the contraction, above (or beneath) the other motionless layer. It is also possible for the forcing to overcome completely the internal hydraulic control. In this limiting situation, if the upstream reservoir is homogeneous, fronts form and the single flowing layer fills the contraction. If the upstream reservoir has two layers, both layers flow in the same direction.

The single-layer flows resulting from moderate and strong barotropic components

represent a special condition which we refer to as 'box flows', in which the presence of a rigid lid directly influences the interfacial shape and position. The inverted box flow corresponds to the situation encountered in an arrested, frictionless salt wedge, where the position and shape of a saline intrusion at the mouth of an estuary is governed not by interfacial entrainment and friction but by the channel width and the flow rate.

Integration of the solutions for periodic flows allows parametrization of two-way exchange, averaged over the barotropic cycle. The integration leads to a parametrization of the exchange as a function of tidal amplitude which may be used in practical examples such as tidally forced exchange through a strait.

We are indebted to Grace Kamitakahara-King and Sharon Yamasaki for carrying out the numerical calculations and to Dr Donald Booth for his assistance with the numerical analysis. We are also indebted to two reviewers, David Wilkinson and an anonymous one, for many helpful comments. All calculations were done independently at the Institute of Ocean Sciences and Scripps Institution of Oceanography. This work received partial support from the Office of Naval Research.

### Appendix. The influence of reservoir conditions

If a reservoir has two layers, maximal exchange requires the existence of stationary bores separating the subcritical reservoirs from the supercritical flows near the controls. Submaximal exchange occurs when the reservoir interface height is such that a bore can move back into and flood the control. The requirement for maximal exchange is that the reservoir interface height on the right  $(y_{2r})_R$  must be greater than, and the reservoir interface on the left  $(y_{2r})_L$  must be less than, the interface height at the virtual control:

$$\left. \begin{array}{l} (y_{2r})_R > y_{2v}, \\ (y_{2r})_L < y_{2v} \end{array} \right\} \text{ for maximal exchange.} \quad (\text{A } 1)$$

In other words, a virtual control must occur for maximal exchange. The limiting interface height on the left is that for which the solution just touches the virtual control condition and then returns to the origin along the straight line  $F_1^2/F_2^2 = \text{constant}$  (see figure 4).

Figure 5 may be used to determine whether or not the virtual control is lost in any practical application. Over the range of  $U_o$  encountered, for example during a tidal cycle, limiting values of the reservoir interface heights (A 1) may be found by inspection. If the reservoir interface heights lie outside these bounds for some portion of the tidal cycle the exchange is influenced by the appropriate reservoir condition. Equations (13*a-i*) must then be replaced by the corresponding equations in the absence of a virtual control, since it is now the reservoir condition, together with the narrowest section, which control the flow:

$$\frac{u_{10}^2}{y_{10}} + \frac{u_{20}^2}{y_{20}} = 1, \quad y_{10} + y_{20} = 1, \quad (\text{A } 2a, b)$$

$$\frac{1}{2}(u_{20}^2 - u_{10}^2) + y_{20} = y_{2r}, \quad U_o = u_{10}y_{10} + u_{20}y_{20}. \quad (\text{A } 2c, d)$$

Equations (A 2*a-d*) may be solved for given values of  $U_o$  and  $y_{2r}$ . The relevant reservoir interface height is that which occurs on the upstream side of the control, which is also the side on which the virtual control is lost. We identify these interface

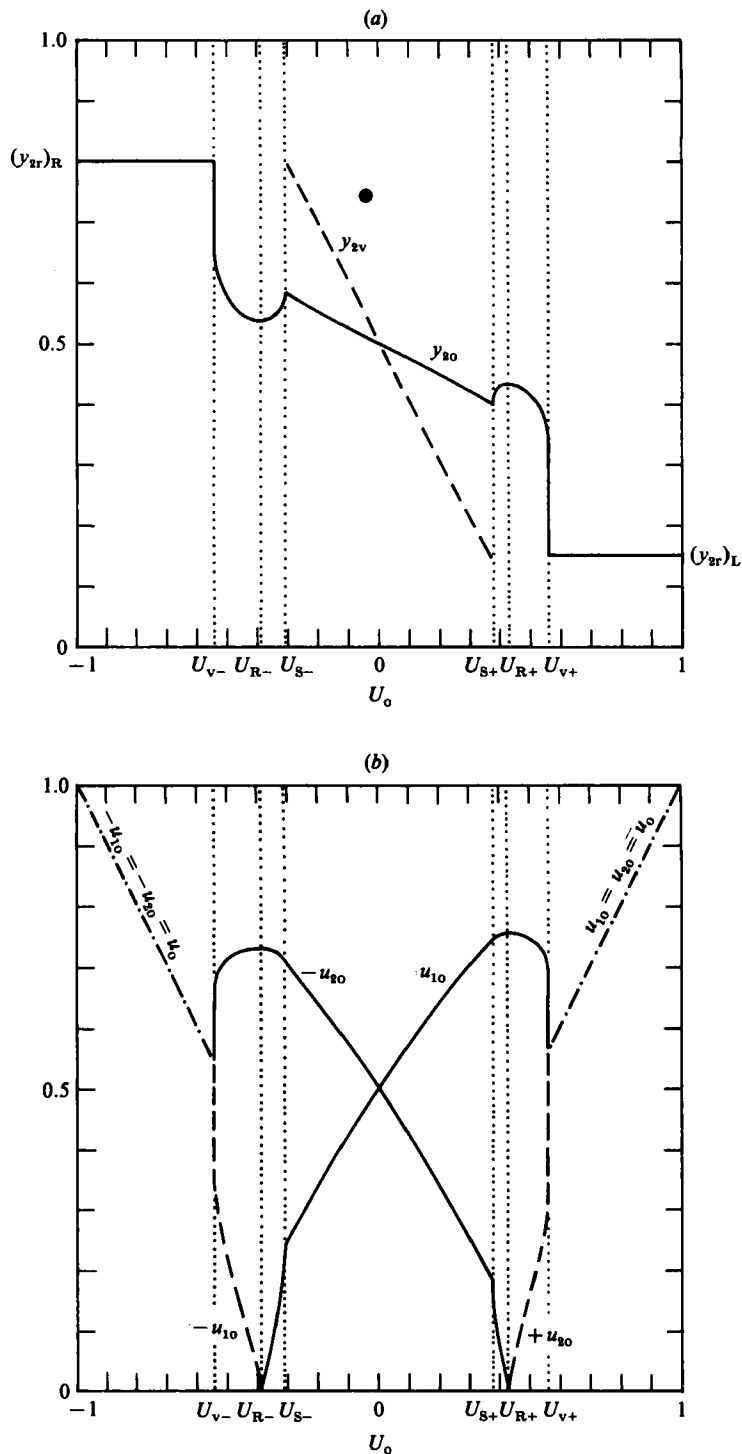


FIGURE 15. (a) Specific example of submaximal exchange flow, with  $(y_{2r})_R = 0.15$  and  $(y_{2r})_L = 0.80$ . For  $U_0$  outside the range  $U_{S-}$  to  $U_{S+}$ , the appropriate reservoir condition influences the exchange rate. For  $U_0$  outside the range  $U_{R-}$  to  $U_{R+}$ , both layers flow in the same direction. (b) Flow speeds  $u_{10}$ ,  $u_{20}$  at the narrowest section for the submaximal-exchange flow example above.

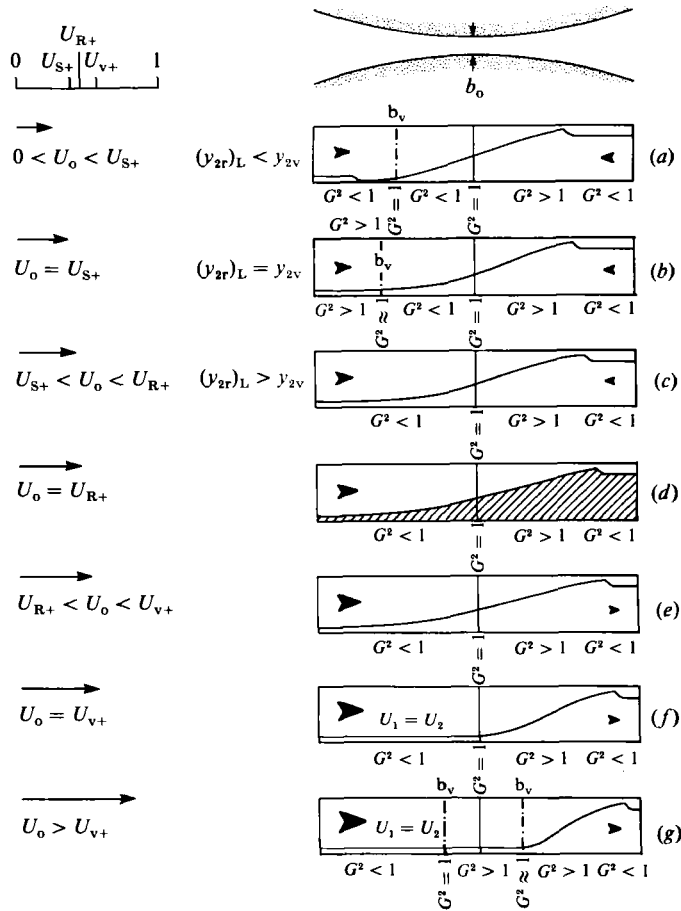


FIGURE 16. Sketches of interface shape for a submaximal-exchange flow with barotropic flow from the left; corresponding sketches for flow from the right would be similar.

heights as  $(y_{2r})_L$ ,  $(y_{2r})_R$  for the left and right reservoirs, together with the corresponding barotropic speeds  $U_{S+}$  and  $U_{S-}$  respectively. Figure 15(a) shows how these limiting values are found for a specific example, together with values of  $y_{20}$  derived from (A 2). The corresponding values of  $u_{10}$ ,  $u_{20}$  are shown in figure 15(b). If the barotropic component is sufficient to arrest the flow in one layer, a new transition  $U_R$  is reached above which both layers flow in the same direction. This transition to ‘Reverse flow’ is obtained by setting  $u_{10} = 0$  in (A 2):

$$U_{R+} = (\frac{2}{3}y_{1r})^{\frac{3}{2}} \text{ for } U_o < 0, \tag{A 3}$$

$$U_{R-} = -(\frac{2}{3}y_{2r})^{\frac{3}{2}} \text{ for } U_o < 0. \tag{A 4}$$

Sketches of the interface shape during periodic flow through these transitions are shown in figure 16. Figure 16(a) represents the maximal-exchange flow analogous to moderate barotropic flow as shown in figure 9, except that we show stationary bores separating the reservoir from the controls. At  $U_o = U_{S+}$ , the virtual control merges with the bore on the upstream side (left) and the reservoir interface height on the left just matches the maximal-exchange control condition (figure 16b). Two-way submaximal exchange occurs for  $U_o$  between  $U_{S+}$  and  $U_{R+}$  (figure 16c). At  $U_o = U_{R+}$ ,



the deeper layer is motionless (figure 16*d*); this solution corresponds to the straight-line solution that lies along the  $F_2^2$ -axis in figure 4. In figure 16(*e*), both layers move in the same direction. The solution in this case is similar to that for figure 16(*c*), which is a submaximal solution, except that the flow is unidirectional. In figure 16(*f*), with  $U_0 > U_{v+}$ , a virtual control analogous to that in figure 16(*b*) appears, but for the unidirectional flow. Finally, in figure 16(*g*), the virtual control occurs upstream with increasing  $U_0$  and the flow on the downstream side adjusts to the downstream reservoir condition via a stationary internal bore. These unidirectional flows have been discussed in detail by Armi (1985).

## REFERENCES

- ARMI, L. 1986 The hydraulics of two flowing layers with different densities. *J. Fluid Mech.* **163**, 27–58.
- ARMI, L. & FARMER, D. 1985 The internal hydraulics of the Strait of Gibraltar and associated sills and narrows. *Oceanologica Acta* **8**, 37–46.
- ASSAF, G. & HECHT, A. 1974 Sea straits: a dynamical model. *Deep-Sea Res.* **21**, 947–958.
- BENJAMIN, T. B. 1968 Gravity currents and related phenomena. *J. Fluid Mech.* **31**, 209–248.
- BRYDEN, H. L. & STOMMEL, H. M. 1984 Limiting processes that determine basic features of the circulation in the Mediterranean Sea. *Oceanologica Acta* **7**, 289–296.
- CHOW, V. T. 1959 *Open-Channel Hydraulics*. McGraw-Hill. 680 pp.
- DYER, K. R. 1973 *Estuaries: A Physical Introduction*. John Wiley & Sons. 140 pp.
- FARMER, D. & ARMI, L. 1986 Maximal two-layer exchange over a sill and through the combination of a sill and contraction with barotropic flow. *J. Fluid Mech.* **164**, 53–76.
- LONG, R. R. 1956 Long wave in a two-fluid system. *J. Met.* **13**, 70–74.
- MURRAY, S. P., HECHT, A. & BABCOCK, A. 1984 On the mean flow in the Tiran Strait in winter. *J. Mar. Res.* **42**, 265–287.
- STOMMEL, H. & FARMER, H. G. 1952 Abrupt change in width in two-layer open channel flow. *J. Mar. Res.* **11**, 205–214.
- STOMMEL, H. & FARMER, H. G. 1953 Control of salinity in an estuary by a transition. *J. Mar. Res.* **12**, 13–20.
- WOOD, I. R. 1970 A lock exchange flow. *J. Fluid Mech.* **42**, 671–687.